

Damping as a function of pulsed field amplitude and bias field in thin film Permalloy

J. P. Nibarger,^{a)} R. Lopusnik, and T. J. Silva
National Institute of Standards and Technology, Boulder, Colorado 80305

(Received 21 November 2002; accepted 5 February 2003)

We have measured the step response in thin film Permalloy as a function of both a hard-axis pulsed field amplitude and an easy-axis longitudinal magnetic bias field using a pulsed inductive microwave magnetometer. The bias field ranged from 0 to 8000 A/m (0 to 100 Oe) and the pulsed field varied from 0.32 to 320 A/m (0.004 to 4 Oe). The rotation angle of the equilibrium magnetization direction varied from 0.002° to 40° for this range of field values. Data were analyzed to extract the Gilbert damping parameter, α . The damping parameter decreased monotonically with an increase in longitudinal bias field. However, there is no observed dependence of α on the pulse amplitude, indicating that the damping is independent of the angle of rotation. We conclude that there is no significant nonlinear generation of spin waves that affects the damping in the case of free induction decay for the range of field pulses employed. [DOI: 10.1063/1.1564866]

As the bandwidth of magnetoelectronic devices approaches microwave frequencies, the role of damping in the switching response of magnetic thin films becomes ever more important. Details of the intrinsic mechanism underlying damping in metallic thin films remain unclear, despite extensive study.¹⁻⁴ The experimental conditions in which the damped gyromagnetic motion is observed can strongly affect the value for the damping rate extracted. In particular, damping effects in a continuous wave (cw) ferromagnetic resonance (FMR) experiment are different from those in a free induction decay experiment in response to a field pulse. For example, it is well established that the FMR linewidth is strongly broadened when large rf exciting powers are employed.⁵ This effect was explained by Suhl as the result of nonlinear generation of spin waves due to an inherent instability of the uniform FMR mode at large precession angles.⁶ An estimate for the instability in Permalloy at 9 GHz (based upon quantum mechanical transition probabilities) yields a maximum FMR precession angle of 2° – 4° , above which first-order Suhl instability leads to premature saturation of the resonance.⁴ However, in a free induction decay experiment, energy is not supplied at a constant rate to drive the uniform precessional mode, thereby precluding application of standard Suhl theory. It is therefore difficult to estimate the excitation levels required to cause spin-wave instability for high speed magnetization switching. Experimental data are required to assess whether such effects have any bearing on the free induction decay geometry.

We present data on the effect of field pulse energy on the damping in a free induction decay geometry where the field pulse is applied along the hard axis of a sample that exhibits uniaxial anisotropy. The magnetization is rotated by angles well in excess of the spin-wave instability in FMR, but no evidence is observed of any nonlinear dependence of damping on the pulse amplitude. For free induction decay, we surmise that the intrinsic damping in permalloy is sufficiently large to damp any precessional motion before any

spin-wave instabilities has a chance to grow to measurable levels.

Three thicknesses of polycrystalline Permalloy films were deposited on sapphire coupons $1\text{ cm} \times 1\text{ cm} \times 100\ \mu\text{m}$ with (0001) orientation. Prior to deposition, the sapphire substrates were cleaned using ion milling in Ar/O₂ and Ar atmospheres to remove contaminants. A dc magnetron operating in an Ar atmosphere at 0.533 Pa (4 mTorr) was used to sputter a 5 nm Ta adhesion layer, followed by 10, 25, and 50 nm of Permalloy (Ni₈₁Fe₁₉). A capping layer of 5 nm of Cu was used to protect the Permalloy from oxidation. Samples were grown in a 20 kA/m external magnetic field to induce uniaxial anisotropy. The base pressure in the deposition chamber was 1.33×10^{-6} Pa (10^{-8} Torr).

Samples were characterized using an induction-field loop to verify their quality. Figure 1 shows typical hard- and easy-axis hysteresis loops. The effective magnetization, M_{eff} , for the purpose of precessional response, was determined as the field applied perpendicular to the sample sur-

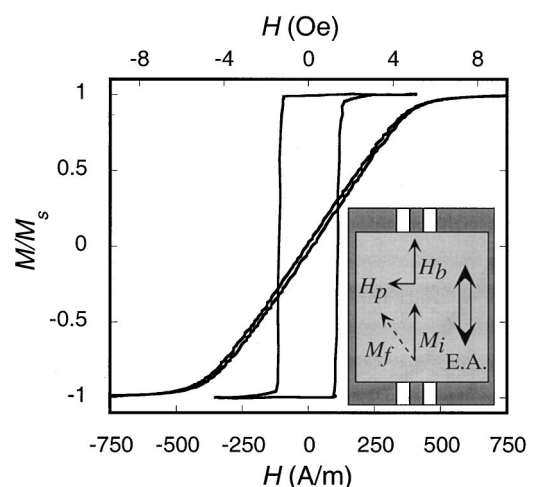


FIG. 1. An easy-axis bias of 32 A/m (0.4 Oe) was needed to close the hard-axis loop. The measurement geometry of the PIMM is shown in the inset with the easy axis of the sample parallel to the waveguide's center conductor. Bias field is applied parallel to the easy axis while a 10 ns pulse field is applied perpendicular to it.

^{a)}Electronic mail: nibarger@boulder.nist.gov

face necessary to saturate the sample. M_{eff} is defined as the saturation magnetization, M_s , decreased by surface anisotropy, K_s :

$$M_{\text{eff}} = M_s - \frac{2K_s}{\mu_0 M_s \delta}, \quad (1)$$

where μ_0 is the permeability of vacuum and δ is the film thickness. Thus, for positive surface anisotropy that exerts torque to rotate the magnetization out of the film plane, the effective magnetization is less than the actual saturation magnetization. Measurements were made with an alternating gradient magnetometer in which M_{eff} was found to be 750, 810, and 846 kA/m (9425, 10 180, and 10 630 Oe) for 10, 25, and 50 nm films, respectively.

Samples were measured using a pulsed inductive microwave magnetometer (PIMM).⁷ The width of the center conductor of the 50 Ω coplanar waveguide used was 450 μm . The easy axis of the sample was aligned parallel to the axis of the waveguide, as shown in the inset of Fig. 1. Field pulses of 50 ps rise time and 10 ns duration were created with a pulse generator. The pulsed field was therefore oriented along the hard axis of the sample. Pulse amplitudes were varied from 10 mV to 10 V using high-bandwidth attenuator networks. The sample was placed on the waveguide with the substrate acting as a 100 μm spacer between the Permalloy films and the waveguide. The nominal field amplitudes were 0.16–160 A/m (0.002–2 Oe), using the Karluquist equation⁸ for the fields from a current strip. Twofold enhancement of the pulsed field amplitude was achieved by placing a floating ground plane above the sample, which increased the pulsed field to 0.32–320 A/m (0.004–4 Oe). The copper–beryllium floating ground plane was the same size as the sample (1 cm \times 1 cm) and was placed directly on top of the sample that is on top of the waveguide. Image currents generated in the ground plane increased instrument sensitivity, as well as the field strength, resulting in a fourfold increase in overall signal-to-noise ratio without any measurable degradation in instrument bandwidth.

Time-resolved precessional response was measured using a 20 GHz bandwidth digital sampling oscilloscope. Data were obtained for easy-axis static fields from 0 to 8 kA/m (0 to 100 Oe) and hard-axis step fields from 0.32 to 320 A/m (0.004 to 4 Oe). The corresponding precession frequencies ranged from about 700 MHz to 3 GHz, and were well within the bandwidth of the detection system.⁷ Field inhomogeneity of the bias field was less than 1% over the sample area. A saturating field of 2.4 kA/m (30 Oe) was applied along the hard axis to obtain a saturated background reference response. The unsaturated and saturated responses were subtracted to obtain the precessional dynamics of the sample.

The induced voltage of the precessional response measured in the time domain was converted into frequency spectra by fast Fourier transform for further analysis. The resonance of the signal was extracted from the zero crossing of the real part of the spectrum and the damping was measured as the full width at half maximum of the imaginary part of the spectrum. The resonance frequency as a function of the bias field can be described by the Kittel formula.⁹ In the limit of uniaxial anisotropy field $H_k + H_b \ll M_{\text{eff}}$, the Kittel formula gives

$$\omega_0^2 = \omega_M \gamma \mu_0 H_b + \omega_M \omega_k, \quad (2)$$

where $\omega_M = \gamma \mu_0 M_{\text{eff}}$, $\omega_k = \gamma \mu_0 H_k$, $\gamma = g \mu_B / \hbar$ is the gyromagnetic ratio, g is the spectroscopic Landé g -factor, μ_B is the Bohr magneton, \hbar is the Planck constant divided by 2π , and μ_0 is the permeability of vacuum. Since M_{eff} was determined independently by static magnetometry, the slope of the data for ω_0^2 vs H_b can be used to extract the Landé g -factor, and the x intercept yields the uniaxial anisotropy H_k value.

The phenomenological damping parameter α refers to the Gilbert damping term in the Landau–Lifshitz–Gilbert equation,¹⁰

$$\frac{d\mathbf{M}}{dt} = \gamma \mu_0 \mathbf{M} \times \mathbf{H} + \frac{\alpha}{M_s} \left(\mathbf{M} \times \frac{d\mathbf{M}}{dt} \right), \quad (3)$$

where \mathbf{H} is the total effective field. For each pulse amplitude, the easy-axis bias field was varied from 0 to 8 kA/m in 80 A/m steps (0 to 100 Oe in 1 Oe steps) yielding a value for the resonance frequency and the full width at half maximum resonance linewidth, $\Delta\omega$, for each bias field. The damping was calculated from $\alpha \approx \Delta\omega / (\gamma \mu_0 M_{\text{eff}})$ within the limit of $M_{\text{eff}} \gg H_b + H_k$.^{11,12} These results agree with damping values obtained by a time-domain fit to the Gilbert equation.⁷ The resonance frequency data were fitted to Eq. (2) and yielded values of H_k for the 10, 25, and 50 nm samples of 424, 480, and 528 A/m (5.3, 6.0, and 6.6 Oe), respectively. The root mean square (rms) variance in the extracted anisotropies was less than 10 A/m as determined by the error in the fitting parameters for Eq. (2).

The extracted values of α for 10, 25, and 50 nm Permalloy are shown in Figs. 2(a)–2(c), respectively. Data are shown as a function of the pulse amplitude for values of H_b of 0, 400, 1600, and 8000 A/m (0, 5, 20, and 100 Oe).

If there were any generation of inhomogeneous precessional motion during the rotation process, this is *by definition* spin-wave generation. Such spin-wave generation would necessarily contribute to the damping rate by removing precessional energy from the uniform excitation mode with $k \approx 0$ to higher order modes with $k \neq 0$. The higher order modes couple poorly to the waveguide with an inductive efficiency that scales inversely with k . In essence, the generation of magnons with $k \neq 0$ is a form of inhomogeneous line broadening that directly contributes to the observed damping, even though such mechanisms do not directly contribute to the draining of precessional energy from the spin system. Thus, we should expect that the damping would be strongly affected by the pulse amplitude if an instability in the precessional dynamics caused a nonlinear increase in spin-wave generation.

Figures 2(a)–2(c) show that there is no dependence of α on the pulse amplitude for any of the thicknesses studied. However, there is a strong dependence of α on H_b . This is explicitly shown for the 25 nm film in the inset of Fig. 2(a) for 320 and 3.2 A/m (4 and 0.04 Oe) pulse fields. This is in agreement with previously reported results.^{7,13–15} It appears that the damping depends on the frequency of the rotational precession rather than on the angle of magnetization rotation.

The final magnetization angle ϕ_f after a field step of amplitude H_p is given by the transcendental equation¹⁶

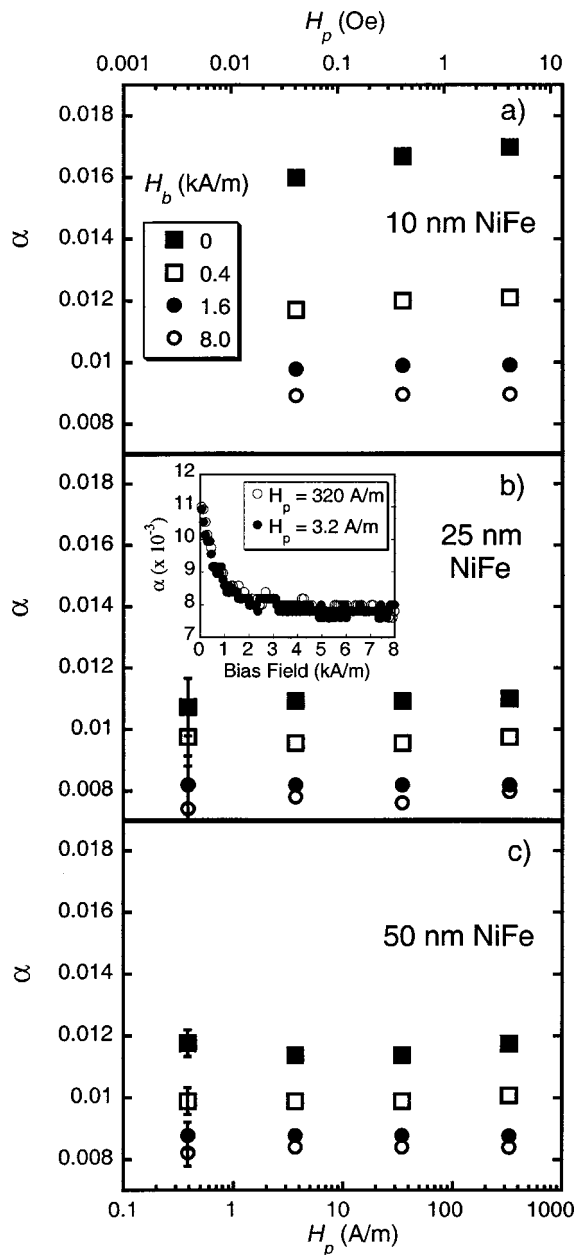


FIG. 2. Dependence of the Gilbert phenomenological damping parameter α with pulse amplitude H_p at 0, 0.4, 1.6, and 8.0 kA/m (0, 5, 20, and 100 Oe) longitudinal bias fields H_b , shown for 10, 25, and 50 nm films in (a)–(c), respectively. The error bars are no larger than the size of the data points unless shown. The inset of (b) is a plot of the damping vs H_b for 320 and 3.2 A/m (4 and 0.04 Oe) pulse fields for the 25 nm thick film.

$$\sin(\phi_f) + \frac{H_b}{H_k} \tan(\phi_f) = \frac{H_p}{H_k}. \quad (4)$$

Using measured values of H_k , and $H_b=0$, Eq. (4) gives rotations of 0.04° – 40° for the 25 nm sample. This large variation shows that the rotation angle itself has no measurable impact on the damping observed. Similarly, for a given nonzero value of bias field, damping is still unaffected by the field pulse amplitude. Thus, we find no evidence of spin-wave instability in these reorientation experiments.

If any other mechanism for nonlinear spin-wave generation (e.g., three magnon processes) were a significant factor that contributed to damping, strong dependence of the damp-

ing on H_p should be observed. This is because the rotation angle is a measure of the number of $k \approx 0$ magnons, N_0 , initially generated in the sample.⁴ For $H_b=0$, N_0 scales quadratically with field pulse¹⁷

$$N_0 = \frac{1}{2g\mu_b} \sqrt{\frac{M_s}{H_k}} H_p^2. \quad (5)$$

Thus, any nonlinear processes for damping for which the relaxation rate scales as some power of the initially excited magnon density should exhibit a quadratic dependence on the pulse amplitude, at the very least. This was not observed.

Nonlinear properties may also be detected through any shifts of H_k or the Landé g -factor when analyzed using Eq. (2). We found no variation of H_k or of the Landé g -factor with the pulse amplitude, further demonstrating that there was no shift of frequency due to nonlinear processes.⁴

These results would suggest that the uniform precessional motion ceases before any nonlinear instabilities have a chance to grow to significant levels. However, our observations do not preclude either nonlinear effects due to saturation of the lowest order modes excited by a waveguide of finite width,⁷ or the generation of spin waves due to rotation of the magnetization from the hard to the easy axis.¹⁸ The pulse amplitudes used in this study were well below the magnitude required to induce a full 90° rotation of the magnetization, thereby avoiding any classical saturation effects.⁵ In addition, this study was limited to the case of dynamic reorientation of the magnetization away from the easy axis in order to compare it with similar magneto-optic measurements that suggest linear response in this configuration.¹⁸

The dependence of the damping parameter on the bias field remains unexplained, although previous studies have attributed the dependence to sample inhomogeneity.^{13,15,19} However, a comparison of the damping parameter of inductive and optical methods showed that the field dependence does not scale with the sample area measured.³

¹ C. E. Patton, J. Appl. Phys. **39**, 3060 (1968).

² R. D. McMichael, M. D. Stiles, P. J. Chen, and W. F. Egelhoff, Jr., Phys. Rev. B **58**, 8605 (1998).

³ T. J. Silva and T. M. Crawford, IEEE Trans. Magn. **35**, 671 (1999).

⁴ M. Sparks, *Ferromagnetic Relaxation Theory* (McGraw-Hill, New York, 1964).

⁵ N. Bloembergen and S. Wang, Phys. Rev. **93**, 72 (1954).

⁶ H. Suhl, J. Phys.: Condens. Matter **1**, 209 (1957).

⁷ T. J. Silva, C. S. Lee, T. M. Crawford, and C. T. Rogers, J. Appl. Phys. **85**, 7849 (1999).

⁸ O. Karlquist, Trans. R. Inst. Tech. Stockholm **86**, 3 (1954).

⁹ C. Kittel, *Introduction to Solid State Physics*, 7th ed. (Wiley, New York, 1995).

¹⁰ Transaction of the Royal Institute of Technology Stockholm

¹¹ D. O. Smith, J. Appl. Phys. **29**, 264 (1958).

¹² N. X. Sun, S. X. Wang, T. J. Silva, and A. B. Kos, IEEE Trans. Magn. **74**, 146 (2002).

¹³ P. Wolf, J. Appl. Phys. **32**, 955 (1961).

¹⁴ T. M. Crawford, T. J. Silva, C. W. Teplin, and C. T. Rogers, Appl. Phys. Lett. **74**, 3386 (1999).

¹⁵ T. J. Klemmer, K. A. Ellis, and B. van Dover, J. Appl. Phys. **87**, 5846 (2000).

¹⁶ E. C. Stoner and E. P. Wohlfarth, Philos. Trans. R. Soc. London, Ser. A **240**, 599 (1948).

¹⁷ H. B. Callen, J. Phys.: Condens. Matter **4**, 256 (1958).

¹⁸ T. J. Silva, P. Kabos, and M. R. Pufall, Appl. Phys. Lett. **81**, 2205 (2002).

¹⁹ G. M. Sandler, H. N. Bertram, T. J. Silva, and T. M. Crawford, J. Appl. Phys. **85**, 5080 (1999).